PHYSICAL REVIEW D **78,** 054014 (2008)

Possible contributions to $e^+e^- \to J/\psi + \eta_c$ due to intermediate meson rescatterings

Yuan-Jiang Zhang,[1,3] Qiang Zhao,[1,2,4] and Cong-Feng Qiao[3,4]

[1]*Institute of High Energy Physics, Chinese Academy of Sciences, Beijing 100049, People's Republic of China*
[2]*Department of Physics, University of Surrey, Guildford, GU2 7XH, United Kingdom*
[3]*Graduate University of Chinese Academy of Sciences, Beijing, 100049, China*
[4]*Theoretical Physics Center for Science Facilities, CAS, Beijing 100049, China*

(Received 25 June 2008; published 15 September 2008)

Inspired by the obvious discrepancies between experiment and nonrelativistic QCD (NRQCD) studies of $e^+e^- \to J/\psi + \eta_c$ at $\sqrt{s} \simeq 10.6$ GeV, we investigate contributions from intermediate meson loops as long-range interaction transitions to this process. The intermediate meson loops include $D\bar{D}(\bar{D}^*)$, $D\bar{D}^*$ (D *or* D^*), $D^*\bar{D}^*(D)$, and corresponding D_s intermediate mesons. With the constraints from experimental data on the vertex couplings, we find that the intermediate meson loops account for $2.7 \sim 6.7$ fb of the cross sections within a reasonable range of cutoff energies of the factor parameter. We also investigate contributions from the absorptive part and find that it accounts for approximately $0.58 \sim 1.38$ fb. These results imply that contributions from long-range interaction transitions may still play a role in such an energy region.

DOI: 10.1103/PhysRevD.78.054014 PACS numbers: 13.66.Bc, 12.38.Lg, 14.40.Gx

I. INTRODUCTION

Recently, one of the hottest topics is the significant discrepancies between experimental and theoretical results for exclusive double-charmonium production $e^+e^- \to J/\psi + \eta_c$ at the center mass energy of 10.58 GeV. In 2002, Belle Collaboration first reported the exclusive cross section for $\sigma[e^+e^- \to J/\psi + \eta_c] \times \mathcal{B}(\eta_c \to \geq 4 \text{ charged}) = 33^{+7}_{-6} \pm 9$ fb [1]. In 2004, Belle Collaboration updated their results $\sigma[e^+e^- \to J/\psi + \eta_c] \times \mathcal{B}(\eta_c \to > 2 \text{ charged}) = 25.6 \pm 2.8 \pm 3.4$ fb [2] and *BABAR* Collaboration also measured the same quantity and found $\sigma[e^+e^- \to J/\psi + \eta_c] \times \mathcal{B}(\eta_c \to > 2 \text{ charged}) = 17.6 \pm 2.8 \pm 2.1$ fb [3].

Theoretically, based on the nonrelativistic QCD (NRQCD) factorization approach [4] at leading order (LO) in the QCD coupling constant (α_s) and charm-quark relative velocity (v), the predictions given by Braaten and Lee [5], Liu, He, and Chao [6], and Hagiwara, Kou, and Qiao [7] are about $2.3 \sim 5.3$ fb, which are about 1 order of magnitude smaller than the experimental measurements. In order to solve this puzzle, many solutions have been proposed. In Ref. [8], the authors consider the corrections of next-to-leading order (NLO) in α_s, which enhanced the cross section with a K factor (the ratio of LO plus NLO to LO) of about $1.8 \sim 2.1$. The authors of Ref. [5] find that including relativistic corrections (order of v^2) will lead to the $K \sim 2.0^{+10.9}_{-1.1}$, but with large uncertainties already bared with the NRQCD matrix elements. In order to reduce the uncertainties of the order-v^2 matrix elements, a potential model is applied to calculate the quarkonium wave function [9], by which the relativistic correlations and corrections of NLO in α_s can be treated [10], and a cross section of 17.5 ± 5.7 fb is obtained. In Ref. [11], the authors present their results by the resummation of relativistic corrections which contains several refinements, such as nonperturbative NRQCD matrix elements, inclusion of the effects of the running of α_s, etc. They conclude that the discrepancies between the theoretical and experimental can be understood. By determining the matrix elements in a different way, Ref. [12] obtains a value of 20.04 fb. A complete computation of LO and NLO contributions were recently presented by Gong and Wang [13], which is a direct confirmation of the results from Ref. [8]. Treatments with light-front approach such as [14–17] and Bethe-Salpeter formalism [18] also provide other possible solutions.

In brief, the present theoretical studies show that NLO contributions turn out to be important in this double-charmonium production, which simultaneously raises concerns about the perturbation expansion. On the other hand, large contributions from NLO corrections suggest that nonperturbative mechanisms may start to play a role. This corresponds to the long-range part of the strong interactions, among which intermediate meson loops could be a natural explanation for the cross section enhancement in $e^+e^- \to J/\psi + \eta_c$ at $\sqrt{s} \simeq 10.6$ GeV.

Intermediate meson loop (IML), or intermediate meson rescattering [or sometimes it is presented as final-state interaction (FSI) with on-shell approximation], as an important nonperturbative transition has been investigated extensively in heavy meson decays. Cheng *et al.* studied the long-distance rescattering effects in hadronic B decays [19]. From the data accumulated at B factories and CLEO, it was found that soft final-state rescattering effects played an essential role in B physics. In Ref. [20], Liu *et al.* also found that contributions from the hadronic loops turned to be important in charmonium hadronic decays. Recently, a

systematic investigation of the IML effects in quarkonium hadronic decays involving Okubo-Zweig-Iizuka (OZI)-rule violations and isospin breaking reveals that IML plays a role in many places and sometimes can even compete against direct scatterings [21–23].

In $e^+e^- \to J/\psi + \eta_c$, the absorptive contributions via IML are supposed to be present, and they do not interfere with the LO NRQCD transitions. With constraints from an experiment on the effective couplings, we can explore the IML mechanism in $e^+e^- \to J/\psi + \eta_c$.

The paper is organized as follows: In Sec. II, we describe the IML model with effective Lagrangians. The numerical results are given in Sec. III. A discussion and summary are given in Sec. IV.

II. THE MODEL

A. Effective Lagrangians

In reaction $e^+e^- \to J/\psi + \eta_c$, the final J/ψ and η_c can be produced by direct production of two $c\bar{c}$ pairs. This process is taken care of by pQCD transitions. In our model, we consider an indirect production process where J/ψ and η_c are produced by the intermediate meson loops as shown by Fig. 1.

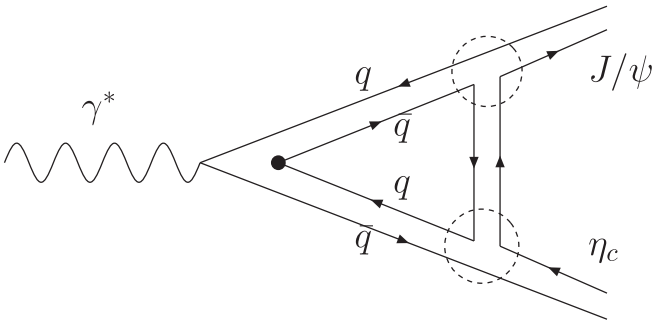

FIG. 1. The schematic diagram for the long-range IML contributions to $J/\psi + \eta_c$ production in e^+e^- annihilation.

In principle, we should include all the possible intermediate meson loops in the calculation. But, the breakdown of the local quark-hadron duality allows us to pick up the leading contributions as a reasonable approximation in the practical calculation [24,25]. Some possible leading IML contributions are shown in Fig. 2. Since those intermediate mesons can be off shell at $\sqrt{s} \simeq 10.6$ GeV, apart from the absorptive part of the loop transition amplitudes, the real part can also contribute. This is different from the FSI approach where only the absorptive amplitudes are considered. In this work, we shall investigate both.

In order to evaluate the diagrams, we adopt the following effective Lagrangians:

$$\begin{aligned}
\mathcal{L}_{\gamma D\bar{D}} &= g_{\gamma D\bar{D}}\{D\partial_\mu\bar{D} - \partial_\mu D\bar{D}\}\mathcal{A}^\mu, \\
\mathcal{L}_{\gamma D\bar{D}^*} &= -ig_{\gamma D\bar{D}^*}\epsilon_{\alpha\beta\mu\nu}\partial^\alpha\mathcal{A}^\beta\partial^\mu\bar{D}^{*\nu}D + \text{H.c.}, \\
\mathcal{L}_{\gamma D^*\bar{D}^*} &= g_{\gamma D^*\bar{D}^*}\{\mathcal{A}^\mu(\partial_\mu D^{*\nu}\bar{D}^*{}_\nu - D^{*\nu}\partial_\mu\bar{D}^*{}_\nu) \\
&\quad + (\partial_\mu\mathcal{A}_\nu D^{*\nu} - \mathcal{A}_\nu\partial_\mu D^{*\nu})\bar{D}^{*\mu} \\
&\quad + D^{*\mu}(\mathcal{A}^\nu\partial_\mu\bar{D}^*{}_\nu - \partial_\mu\mathcal{A}_\nu\bar{D}^{*\nu})\}, \\
\mathcal{L}_{\psi D\bar{D}} &= g_{\psi D\bar{D}}\{D\partial_\mu\bar{D} - \partial_\mu D\bar{D}\}\psi^\mu, \\
\mathcal{L}_{\psi D\bar{D}^*} &= -ig_{\psi D\bar{D}^*}\epsilon_{\alpha\beta\mu\nu}\partial^\alpha\psi^\beta\partial^\mu\bar{D}^{*\nu}D + \text{H.c.}
\end{aligned} \tag{1}$$

where $\mathcal{A}^\mu$ and ψ^μ are photon and J/ψ vector-meson fields, respectively, and D is the pseudoscalar-meson field with $D = (D^0, D^+, D_s^+)$ and $\bar{D} = (\bar{D}^0, D^-, D_s^-)^T$; D^* is the vector-meson field with $D^* = (D^{*0}, D^{*+}, D_s^{*+})$ and $\bar{D} = (\bar{D}^{*0}, D^{*-}, D_s^{*-})^T$. The coupling constants appearing in the above equations will be determined as follows.

For the couplings of photon with D-meson, such as $g_{\gamma D\bar{D}}$, $g_{\gamma D\bar{D}^*}$, $g_{\gamma D^*\bar{D}^*}$, we can extracted them from the experimental data [26]. Applying the effective Lagrangians, the γ couplings can be obtained:

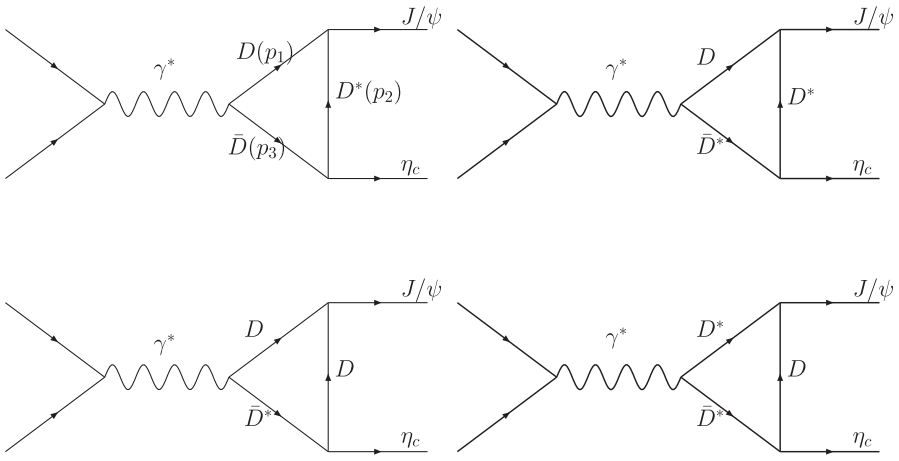

FIG. 2. Some possible leading intermediate meson loops contribute to $e^+e^- \to J/\psi + \eta_c$.

TABLE I. The coupling constants of a photon with D-meson determined in $e^+e^- \to D\bar{D}$, $D\bar{D}^*$, $D^*\bar{D}^*$. The cross sections are taken from Ref. [26].

Coupling constants	Value	Cross section (pb)
$g_{\gamma D\bar{D}}$	4.81×10^{-3}	0.04
$g_{\gamma D\bar{D}^*}$	2.73×10^{-3} GeV^{-1}	0.71
$g_{\gamma D^*\bar{D}^*}$	1.10×10^{-3}	0.65

$$g_{\gamma D\bar{D}} = \left[\frac{3s^{5/2}\sigma_{e^+e^-\to D\bar{D}}}{2\alpha_e|\vec{P}_D|^3}\right]^{1/2},$$
$$g_{\gamma D\bar{D}^*} = \left[\frac{16s^{5/2}\sigma_{e^+e^-\to D\bar{D}^*}}{\alpha_e|\vec{P}_{D^*}|C_{D\bar{D}^*}}\right]^{1/2}, \quad (2)$$
$$g_{\gamma D^*\bar{D}^*} = \left[\frac{16s^{5/2}\sigma_{e^+e^-\to D^*\bar{D}^*}m_{D^*}^4}{\alpha_e|\vec{P}'_{D^*}|C_{D^*\bar{D}^*}}\right]^{1/2},$$

with

$$C_{D\bar{D}^*} = m_{\bar{D}^*}^4 - 2(m_D^2 + s)m_{\bar{D}^*}^2 + (m_D^2 - s)^2 + \tfrac{4}{3}s|\vec{P}_{\bar{D}^*}|^2,$$
$$C_{D^*\bar{D}^*} = s^3 + 6s^2m_{D^*}^2 - 28sm_{D^*}^4 - 48m_{D^*}^6 \quad (3)$$
$$- \tfrac{4}{3}(12m_{D^*}^4 - 6sm_{D^*}^2 + s^2)|\vec{P}'_{D^*}|^2,$$

where $\vec{P}_D$, $\vec{P}_{D^*}$, and $\vec{P}'_{D^*}$ are the final-state three-momentum for the processes $e^+e^- \to D\bar{D}$, $D\bar{D}^*$, $D^*\bar{D}^*$, respectively; $\alpha_e = 1/137$ is the fine-structure constant; σ are the corresponding cross sections. In the SU(3) limit, we have the following relations: $g_{\gamma D_s\bar{D}_s} = g_{\gamma D\bar{D}}$, $g_{\gamma D_s\bar{D}_s^*} = g_{\gamma D\bar{D}^*}$, and $g_{\gamma D_s^*\bar{D}_s^*} = g_{\gamma D^*\bar{D}^*}$. The values are listed in Table I.

For the $J/\psi D\bar{D}^*$ coupling, we use the relation in the heavy quark mass limit [27,28],

$$g_{\psi D\bar{D}^*} = g_{\psi D\bar{D}}/\tilde{M}_D, \quad (4)$$

where $\tilde{M}_D$ is the mass scale of the D/D^* mesons. We adopt the coupling constants $g_{\psi D\bar{D}} = 7.44$ and $g_{\psi D\bar{D}^*} = 3.84$ GeV^{-1} from Ref. [28], and $g_{\eta_c D^*\bar{D}^*} = g_{\psi D\bar{D}}$, $g_{\eta_c D\bar{D}^*} = g_{\psi D\bar{D}^*}$ in the following calculation.

B. Intermediate meson loops contribution

We take $D\bar{D}(\bar{D}^*)$, $D\bar{D}^*$ (D or D^*), $D^*\bar{D}^*(D)$, and corresponding D_s intermediate mesons into account. The transition amplitude for $e^+e^- \to J/\psi + \eta_c$ via intermediate meson loops can be expressed as follows:

$$M_{fi}^{\rm Loop} = \bar{v}^{(s')}(p'_e)(-ie\gamma_\rho)u^s(p_e)\frac{i\varepsilon_\gamma^\rho}{s}\int\frac{d^4p_2}{(2\pi)^4} \times \frac{T_1T_2T_3}{a_1a_2a_3}\mathcal{F}(p_2^2), \quad (5)$$

where $T_{1,2,3}$ are the vertex functions of which the detailed expressions have been given in Refs. [21,22]. We include them in the appendix for all the above-mentioned loops. The four-vector momentum p_2 is for the exchange meson. Variables $a_1 \equiv p_1^2 - m_1^2$, $a_2 \equiv p_2^2 - m_2^2$, and $a_3 \equiv p_3^2 - m_3^2$ are the denominators of the propagators of the intermediate mesons, respectively.

In the above equation a form factor $\mathcal{F}(p_2^2)$ is introduced to take into account the off-shell effects of the exchanged mesons and also kill the divergence of the integrals. The following commonly used form factor is adopted:

$$\mathcal{F}(p^2) = \left(\frac{\Lambda^2 - m_{\rm ex}^2}{\Lambda^2 - p^2}\right)^n, \quad (6)$$

where $n = 0, 1, 2$ correspond to different treatments of the loop integrals. Λ is the cutoff energy, which should not be far away form the physical mass of the exchanged particles. Since there are different particles exchanged in the meson loops, a useful parametrization is as follows [19]:

$$\Lambda = m_{\rm ex} + \alpha\Lambda_{\rm QCD}, \quad (7)$$

where $\Lambda_{\rm QCD} = 220$ MeV and α is a tunable parameter; $m_{\rm ex}$ is the mass of the exchanged meson. This way of parametrizing the cutoff energies is slightly different from the previous works [21–23], where Λ was universal for all the meson loops. Here, the mass differences between the exchanged particles are taken into account. The parameter α will then be constrained by experimental data. In this work, we apply the dipole form factor in the calculation, i.e. $n = 2$. The relation between the loop amplitudes with the dipole and monopole form factors are given in Appendix C.

C. Absorptive contributions from the IML

It is important to examine the absorptive part of the IML transitions. Non-negligible contributions from the absorptive part would be strong evidence for possible long-range transitions in the double-charmonium productions.

Taking $D(p_1)$ [or $D^*(p_1)$] and $\bar{D}(p_3)$ [or $D^*(p_3)$] as on-shell particles, we obtain the absorptive transition:

$$M_{fi}^{\rm Abs} = \frac{1}{2}\bar{v}^{(s')}(p'_e)(-ie\gamma_\rho)u^s(p_e)\frac{i\varepsilon_\gamma^\rho}{s} \times \int\frac{d^3\vec{p}_1}{(2\pi)^3 2E_1}\frac{d^3\vec{p}_3}{(2\pi)^3 2E_3}(2\pi)^4 \times \delta^4(p'_e + p_e - p_1 - p_3)\frac{T_1T_2T_3}{p_2^2 - m_2^2 + im_2\Gamma_2}\mathcal{F}(p_2^2)$$
$$= \bar{v}^{(s')}(p'_e)(-ie\gamma_\rho)u^s(p_e)\frac{i\varepsilon_\gamma^\rho}{s}\int_{-1}^{1}\frac{|\vec{p}_1|d\cos\theta}{16\pi\sqrt{s}} \times \frac{T_1T_2T_3}{p_2^2 - m_2^2 + im_2\Gamma_2}\mathcal{F}(p_2^2), \quad (8)$$

where θ is the angle between $\vec{p}_1$ and $\vec{p}_\psi$. The kinematic definitions have been given in Appendix B. The vertex functions $T_{1,2,3}$ and form factor $\mathcal{F}(p_2^2)$ are the same as the previous definitions.

D. EM transition via $\Upsilon(4S)$ intermediate meson

The present data from Belle were taken at $\sqrt{s} = 10.58$ GeV and 10.52 GeV, respectively. The higher one corresponds to the mass of $\Upsilon(4S)$ while the lower one is a sideband measurement. However, the datum samples are not sufficient for determining the cross section differences between these two energies. Therefore, the role played by $\Upsilon(4S)$ from the present Belle results [1,2,26] is still unclear, and the $\Upsilon(4S) \to J/\psi + \eta_c$ coupling is also unknown. In Ref. [29], exclusive decays of $\Upsilon(4S)$ to double-charmonium states were evaluated and the branching ratio for $\Upsilon(4S) \to J/\psi + \eta_c$ was predicted to be at an order of 10^{-9}. At amplitude level, such a small contribution can still produce some structures at the $\Upsilon(4S)$ mass due to the destructive interference between the resonance strong decay and continuum amplitudes.

In our calculation we take into account the contribution of the $\Upsilon(4S)$. Its interference with the IML amplitudes is useful for us to examine the model dependence of the IML transition and sensitivities of the cross sections to its coupling to $J/\psi\eta_c$.

Fortunately, the EM coupling for $\Upsilon(4S) \to e^+e^-$ has been relatively well measured [30]. We can then determine the $V\gamma^*$ coupling eM_V^2/f_V by the vector-meson dominance (VMD) model [31],

$$\frac{e}{f_V} = \left[\frac{3\Gamma_{V\to e^+e^-}}{2\alpha_e|\mathbf{p}_e|}\right]^{1/2}, \tag{9}$$

where $\Gamma_{V\to e^+e^-}$ is the partial decay width, $|\mathbf{p}_e|$ is the electron three-momentum in the vector-meson rest frame, and $\alpha_e = 1/137$ is the fine-structure constant. It should be noted that this form of interaction is only an approximation and can have large off-shell effects arising from either the off-shell vector meson or virtual photon fields. In this approach we consider such effects in the $V\gamma P$ coupling form factor which will then be absorbed into the energy-dependent widths of the vector mesons.

The transition amplitude that corresponds to Fig. 3 is

$$M_{fi} = \bar{v}^{(s')}(p_e')(-ie\gamma^\alpha)u^s(p_e)\frac{i}{s(s - M_\Upsilon^2 + i\Gamma_\Upsilon M_\Upsilon)} \times \frac{eM_\Upsilon^2}{f_\Upsilon} g_{\Upsilon\psi\eta_c}\varepsilon_{\alpha\beta\mu\nu}p_{\eta_c}^\beta p_\psi^\mu \varepsilon_\psi^\nu.$$

In case the partial width of $\Gamma_{\Upsilon\to\psi\eta_c}$ is available, we can extract the $\Upsilon\psi\eta_c$ coupling via

$$\Gamma_{\Upsilon\to\psi\eta_c} = \frac{g_{\Upsilon\psi\eta_c}^2|\mathbf{p}_\psi|^3}{12\pi}, \tag{10}$$

where $|\mathbf{p}_\psi|$ is the three-momentum of J/ψ in the Υ meson rest frame.

The total transition amplitudes apart from the leading QCD contribution can thus be expressed as

$$M_{fi} = M_{fi}^{\mathrm{EM}} + M_{fi}^{\mathrm{Loop}}. \tag{11}$$

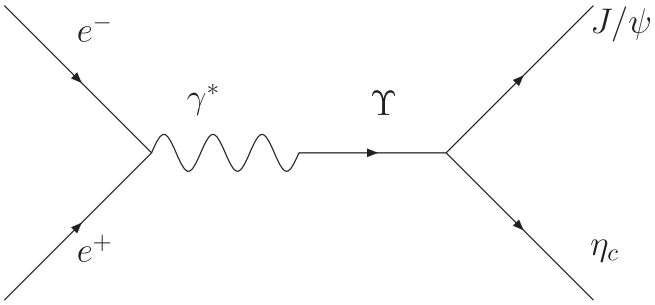

FIG. 3. The $J/\psi + \eta_c$ production via resonance $\Upsilon(4S)$.

We estimate the differential cross section via

$$\frac{d\sigma}{d\Omega} = \frac{1}{64\pi^2 s}\frac{|P_f|}{|P_e|}\frac{1}{4}\sum_{\mathrm{spin}}|\mathcal{M}_{fi}|^2, \tag{12}$$

where p_e is the three-momentum of the initial electron (positron) in the overall center-of-mass (c.m.) system. The mass of the electron has been neglected, i.e. $p_e = E_{\mathrm{cm}}/2$ is applied.

III. NUMERICAL RESULTS

As mentioned before, the present experimental data at $\sqrt{s} = 10.52$ and 10.58 GeV cannot tell the role played by $\Upsilon(4S)$. But we can still define quantity R, which is the $e^+e^- \to J/\psi + \eta_c$ cross section ratio at $\sqrt{s} = 10.52$ GeV to that at $\sqrt{s} = 10.58$ GeV, i.e. $R \equiv \sigma_{10.52}/\sigma_{10.58}$. It is a function of both resonance direct transition and IML amplitudes, and we expect that it should not be sensitive to the cutoff energy introduced to the IML though the exclusive IML contributions may have strong dependence on it. Unfortunately, no information about the $\Upsilon(4S)$ coupling to $J/\psi\eta_c$ is available. We then simply assume $R = 0.5$ at $\alpha = 1.8$ to fix the coupling $g_{\Upsilon\psi\eta_c} = 5.26 \times 10^{-5}$ GeV^{-1}. This corresponds to $\mathrm{BR}(\Upsilon \to J/\psi\eta_c) = 2.9 \times 10^{-7}$. One should not take this value seriously since our strategy here is to fix $g_{\Upsilon\psi\eta_c}$, and then examine the sensitivity of R to the form factor parameter α as a test of the behavior of the IML.

In Fig. 4, by fixing $g_{\Upsilon\psi\eta_c} = 5.26 \times 10^{-5}$ GeV^{-1}, we plot the ratio R with a varying α. It shows that within the commonly accepted range of $\alpha = 1.6 \sim 2.0$, the ratio R varies from 0.43 to 0.57. This is an indication of insensitivity of the loop contributions to the form factors within a reasonable range of the cutoff energy. We also find that such a property is retained even for larger $g_{\Upsilon\psi\eta_c}$. In such a case, the cross section at the mass of $\Upsilon(4S)$ is enhanced by the resonance contribution while the sideband cross section is relatively small. A quantitative determination of the $\Upsilon(4S)$ requires future precise measurements of the cross sections at both $\sqrt{s} = 10.52$ and 10.58 GeV.

We also plot the cross section dependence on α at $\sqrt{s} = 10.52$ and 10.58 GeV in Fig. 5. It shows that these two cross sections increase with α slowly and also appear to be

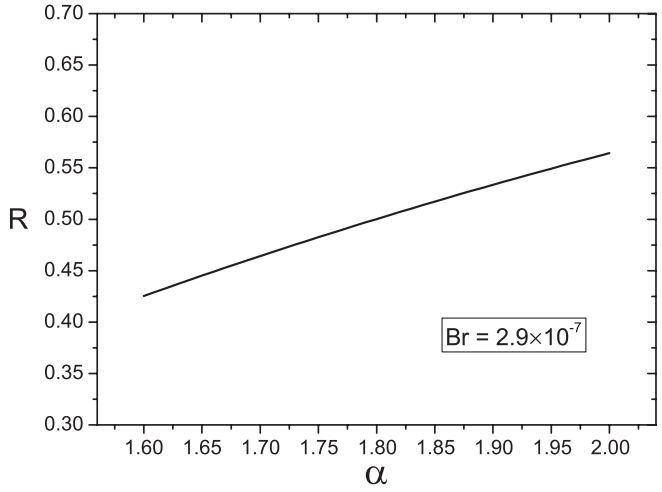

FIG. 4. The sensitivity of R to the form factor parameter α with the $\Upsilon J/\psi\eta_c$ coupling fixed at $R = 0.5$ and $\alpha = 1.8$.

stable. Again the difference between these two cross sections are due to the assumed contribution from $\Upsilon(4S)$.

In Fig. 6, we fix the form factor parameter $\alpha = 1.8$ and then investigate the effects from the $\Upsilon(4S)$ at different R values. The total cross sections from the IML plus resonance $\Upsilon(4S)$ are presented. A smaller value of R corresponds to a larger $g_{\Upsilon\psi\eta_c}$ coupling in the present choice of a constructive relative phase. It is possible that their interference is destructive and a dip will appear at $\sqrt{s} = 10.58$ GeV [29]. In this sense, we emphasize again that it is essential to have precise data for the cross sections at both $\sqrt{s} = 10.52$ and 10.58 GeV.

In Fig. 7, we plot the total cross section again, but with several different α values. The solid curve is the same as that in Fig. 6 with $\alpha = 1.8$. Again, some sensitivities to α are highlighted. We also present the results without $\Upsilon(4S)$, i.e. exclusive cross sections from the IML, as denoted by

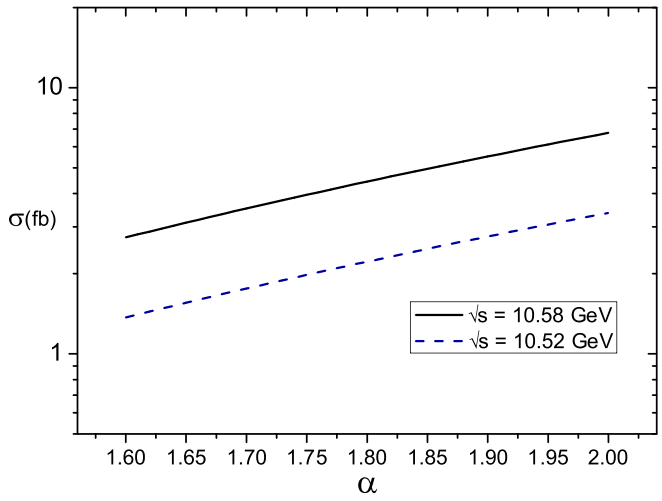

FIG. 5 (color online). Sensitivities of the $e^+e^- \to J/\psi + \eta_c$ cross section to the form factor parameter α at $\sqrt{s} = 10.58$ (solid line) and $\sqrt{s} = 10.52$ GeV (dashed line) with $R = 0.5$.

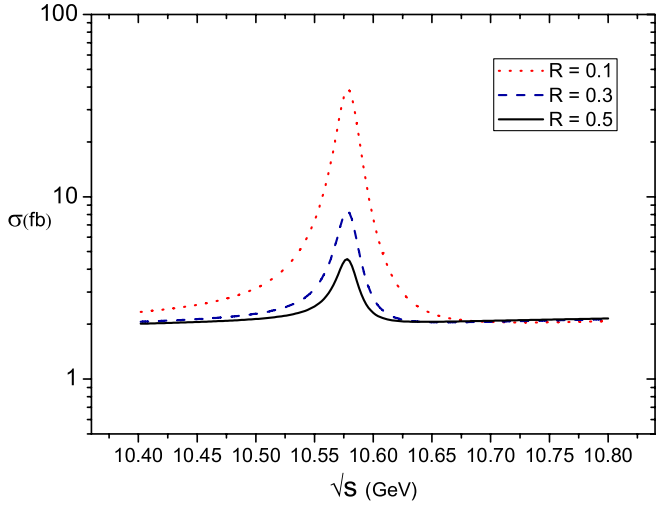

FIG. 6 (color online). The $\sqrt{s}$ evolution of the $e^+e^- \to J/\psi + \eta_c$ cross section with different R values which correspond to different branch ratios for $\Upsilon(4s) \to \psi + \eta_c$. The form factor parameter $\alpha = 1.8$ is adopted.

the dot-dashed curve. A flat behavior is observed along with $\sqrt{s}$.

It is interesting to see that the total cross section without the $\Upsilon(4S)$ has the same order of magnitude as the pQCD leading order results. In Table II we list the total cross sections with different α values. In a range of $\alpha = 1.6 \sim 2.0$ the total cross sections increase from 2.74 fb to 6.76 fb. Eventually, this range is acceptable for the form factor uncertainties which is unavoidable in this effective Lagrangian approach. Similarly, the sideband cross sections at $\sqrt{s} = 10.52$ GeV (i.e. can be viewed as no $\Upsilon(4S)$ contributions) vary from 1.3 fb to 3.1 fb.

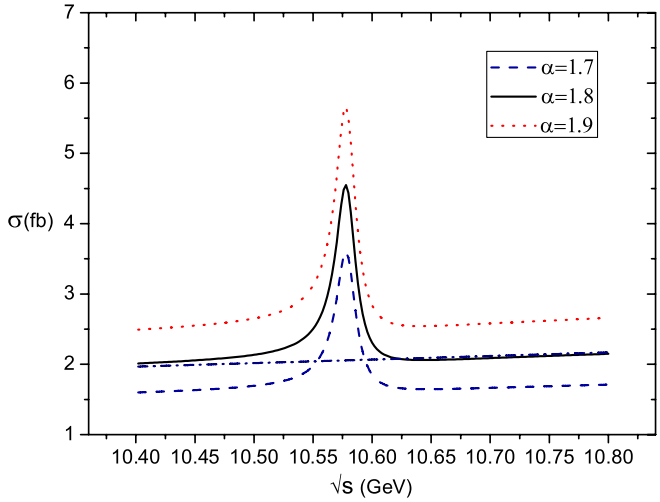

FIG. 7 (color online). The $\sqrt{s}$ evolution of the $e^+e^- \to J/\psi + \eta_c$ cross section with $R = 0.5$ but varying values of $\alpha = 1.7$ (dashed line), 1.8 (solid line), and 1.9 (dotted line). The dot-dashed line denotes the result without the $\Upsilon(4S)$ contribution at $\alpha = 1.8$.

TABLE II. $e^+e^- \to J/\psi + \eta_c$ cross sections with different α values at $\sqrt{s} = 10.58$ GeV. The ratio $R = 0.5$ is applied. σ is the results from the IML with $\Upsilon(4S)$ contribution [σ' without $\Upsilon(4S)$ contribution], while σ_A is from the absorptive transitions where no $\Upsilon(4S)$ is considered.

α	1.6	1.7	1.8	1.9	2.0
$\sigma_{10.58}$ (fb)	2.74	3.52	4.43	5.51	6.76
$\sigma'_{10.58}$ (fb)	1.28	1.64	2.06	2.55	3.11
σ_A (fb)	0.587	0.741	0.924	1.14	1.38

In order to further clarify the role played by the IML, we calculate the absorptive contributions from the loops by making the on-shell approximation for the intermediate mesons. In Fig. 8, the α dependence of the cross section at $\sqrt{s} = 10.58$ GeV is presented. Since the absorptive part will be present in the transition amplitudes, its stability within the commonly accepted range of the form factor parameter turns to be essential for understanding its role in this process. As shown by Fig. 8, with α from 1.6–2.0, the absorptive cross section varies from ~0.6–1.4 fb, and can be regarded as quite stable. We also list the cross sections with different values of α in Table II to compare with the full loop calculations.

We then examine the total absorptive cross sections with fixed α values in Fig. 9. It shows that with $\alpha = 1.8$, the cross section is about 0.924 fb, and its energy dependence is rather weak. Again, larger values for α produce larger cross sections. The most interesting feature is that the absorptive cross sections are nearly the same order of magnitude as the LO results of NRQCD.

One should be cautioned in the understanding of the result of Fig. 9. It eventually reflects the energy dependence of the IML form factors, and with the couplings of $e^+e^- \to D\bar{D}$, etc. fixed at $\sqrt{s} = 10.58$ GeV. In this approach QCD hard interactions have been contained in those couplings derived at $\sqrt{s} = 10.58$ GeV, i.e. $g_{\gamma D\bar{D}}$, $g_{\gamma D\bar{D}^*}$, and $g_{\gamma D^*\bar{D}^*}$. The form factor in Eq. (5) will then take care of the soft interactions arising from the intermediate meson loops. Hence, one should not compare the energy dependence of Fig. 9 with the QCD factorization [8,32] for the direct production of double charmonia.

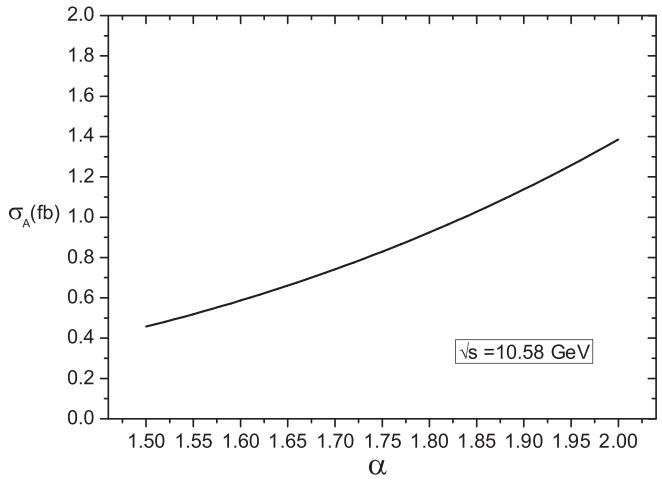

FIG. 8. The α dependence of the absorptive cross sections from the meson loops.

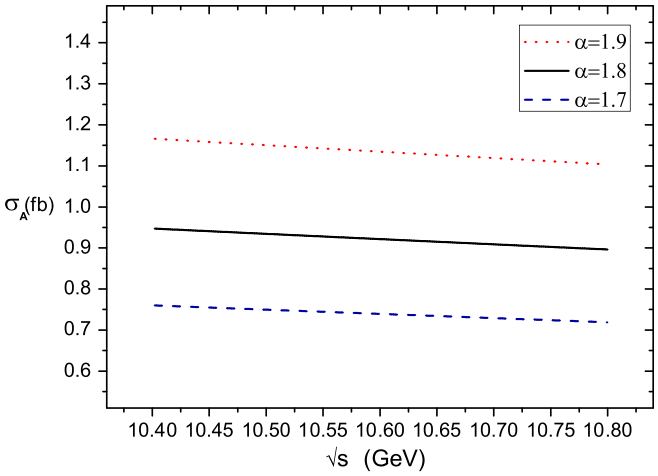

FIG. 9 (color online). The energy evolution of the absorptive cross sections from the meson loops with different α values.

Also, it should be pointed out that the IML contributions as a source of long-range interaction transition are different from the soft exchanges in the pQCD factorization [32]. It is not a full correspondence of the soft QCD. Ideally, we expect that the sum of all the possible intermediate meson loops be equivalent to the soft exchanges in the pQCD factorization according to the quark-hadron duality argument [24,25]. In reality the breakdown of the local quark-hadron duality allows us to pick up the leading IML contributions as a first-order approximation.

IV. SUMMARY

We estimate the intermediate meson loop contributions to $e^+e^- \to J/\psi + \eta_c$ in an effective Lagrangian theory. By applying the available experimental information to the constraints of the meson-meson coupling vertices, we investigate contributions from $D\bar{D}(D^*)$, $D\bar{D}^*(D)$, $D\bar{D}^*(D^*)$, and $D^*\bar{D}^*(D)$. The model dependence mainly comes from the form factors adopted for the loop integrals. Fortunately, it shows that the results do not vary dramatically with the cutoff energies within the commonly accepted range. The resonance $\Upsilon(4S)$ effects are also estimated. Precise measurements of the cross sections at the resonance energy and sideband will be able to provide useful information on the $\Upsilon(4S)$.

In order to clarify the IML contributions, we also calculate the absorptive part of the loops and find that the IML contributes nearly the same order of magnitude as the LO of NRQCD. It is likely that the long-range IML is an important mechanism apart from the NRQCD LO transi-

tions. Qualitatively, the long-range IML transitions may have some overlaps with the NLO processes if they are not obviously suppressed. Note that the IML contributions go to the effective coupling of the antisymmetric tensor at hadronic level. It suggests that the relativistic corrections may also have some overlaps with the IML mechanism. To understand the large cross sections from the experiment, one perhaps should consider both short and long-range transitions to obtain an overall consistent prescription. Again, we emphasize the importance of extracting the precise cross sections at and off resonance $\Upsilon(4S)$.

ACKNOWLEDGMENTS

We would like to thank C. H. Chang, K. T. Chao, T. Huang, Y. Jia, X. Q. Li, S. Olsen, W. Wang, and J. X. Wang for fruitful discussions. We also thank G. Li for double-checking part of the calculations and useful discussions. This work is supported, in part, by the National Natural Science Foundation of China (Grant No. 10675131), Chinese Academy of Sciences (KJCX3-SYW-N2), and the U.K. EPSRC (Grant No. GR/S99433/01).

APPENDIX A: VERTEX FUNCTIONS FOR THE INTERMEDIATE MESON LOOPS

For $D\bar{D}(D^*)$, the vertex functions are

$$\begin{cases} T_1 \equiv ig_1(p_1 - p_3)\cdot\varepsilon_\gamma, \\ T_2 \equiv ig_2\varepsilon_{\alpha\beta\mu\nu}p_\psi^\alpha\varepsilon_\psi^\beta p_2^\mu\varepsilon_2^\nu, \\ T_3 \equiv ig_3(p_{\eta_c} + p_3)\cdot\varepsilon_2, \end{cases} \tag{A1}$$

where g_1, g_2, and g_3 are the coupling constants at the meson interaction vertices (see Fig. 2). The four vectors, $p_{J/\psi}$, and p_{η_c} are the momenta for the final state J/ψ and η_c meson; the four-vector momentum, p_1, p_2, and p_3 are the intermediate mesons, respectively.

As shown by Fig. 2, the vertex functions for the $D\bar{D}^*(D)$ + c.c. loop are

$$\begin{cases} T_1 \equiv if_1\varepsilon_{\alpha\beta\mu\nu}p_3^\alpha\varepsilon_3^\beta p_\gamma^\mu\varepsilon_\gamma^\nu, \\ T_2 \equiv if_2(p_2 - p_1)\cdot\varepsilon_\psi, \\ T_3 \equiv if_3(p_{\eta_c} - p_2)\cdot\varepsilon_3. \end{cases} \tag{A2}$$

where $f_{1,2,3}$ are the coupling constants.

We also consider the transition amplitude from the intermediate $D\bar{D}^*(D^*)$ + c.c. loop, which can be expressed as the following formula:

$$\begin{cases} T_1 \equiv ih_1\varepsilon_{\alpha\beta\mu\nu}p_\gamma^\alpha\varepsilon_\gamma^\beta p_3^\mu\varepsilon_3^\nu, \\ T_2 \equiv ih_2\varepsilon_{\alpha'\beta'\mu'\nu'}p_2^{\alpha'}\varepsilon_2^{\beta'}p_\psi^{\mu'}\varepsilon_\psi^{\nu'}, \\ T_3 \equiv ih_3\varepsilon_{\alpha''\beta''\mu''\nu''}p_2^{\alpha''}\varepsilon_2^{\beta''}p_3^{\mu''}\varepsilon_3^{\nu''}, \end{cases} \tag{A3}$$

where $h_{1,2,3}$ are the coupling constants.

The transition amplitude from the intermediate $D^*\bar{D}^*(D)$ + c.c. loop can be written as Eq. (A4)

$$\begin{cases} T_1 \equiv i\lambda_1[-\varepsilon_\gamma\cdot(p_1 - p_3)\varepsilon_1\cdot\varepsilon_3 + 2p_1\cdot\varepsilon_3\varepsilon_1\cdot\varepsilon_\gamma + 2\varepsilon_1\cdot p_3\varepsilon_\gamma\cdot\varepsilon_3], \\ T_2 \equiv i\lambda_2\varepsilon_{\alpha\beta\mu\nu}p_1^\alpha\varepsilon_1^\beta p_\psi^\mu\varepsilon_\psi^\nu, \\ T_3 \equiv i\lambda_3(p_{\eta_c} - p_2)\cdot\varepsilon_3, \end{cases} \tag{A4}$$

where $\lambda_{1,2,3}$ are the coupling constants.

APPENDIX B: FOUR-VECTOR MOMENTUM EXPRESSIONS AND WAVE FUNCTIONS

In order to calculate the absorptive amplitude of $e^+e^- \to J/\psi + \eta_c$, it is convenient if we choose the overall c.m. frame and choose the z axis along the three-vector momentum of J/ψ. After taking $m_e = m_{e^+} \simeq 0$, we have

$$\begin{cases} p_\psi^\mu = (E_\psi, 0, 0, |\vec{p}_f|)^T, \\ p_{\eta_c}^\mu = (E_{\eta_c}, 0, 0, -|\vec{p}_f|)^T, \\ p_1^\mu = (E_1, |\vec{p}_1|\sin\theta\cos\varphi, |\vec{p}_1|\sin\theta\sin\varphi, |\vec{p}_1|\cos\theta)^T, \\ p_2^\mu = (E_2, -|\vec{p}_1|\sin\theta\cos\varphi, -|\vec{p}_1|\sin\theta\sin\varphi, |\vec{p}_f| - |\vec{p}_1|\cos\theta)^T, \\ p_3^\mu = (E_3, -|\vec{p}_1|\sin\theta\cos\varphi, -|\vec{p}_1|\sin\theta\sin\varphi, -|\vec{p}_1|\cos\theta)^T, \\ p_e^\mu = (E, E\sin\theta_1\cos\varphi_1, E\sin\theta_1\sin\varphi_1, E\cos\theta_1)^T, \\ p_e'^\mu = (E, -E\sin\theta_1\cos\varphi_1, -E\sin\theta_1\sin\varphi_1, -E\cos\theta_1)^T \end{cases} \tag{B1}$$

and

$$\begin{cases} \epsilon_\psi^\mu(\pm 1) = \mp\frac{1}{\sqrt{2}}(0, 1, \pm i, 0)^T, \\ \epsilon_\psi^\mu(0) = (|\vec{p}_f|/M_\psi, 0, 0, E_\psi/M_\psi)^T, \\ u^s(p_e) = \frac{\not{p}_e}{\sqrt{E}}(\chi(s)^T, 0, 0)^T, \\ v^s(p_e') = \frac{-\not{p}_e'}{\sqrt{E}}(0, 0, \chi(s)^T)^T, \end{cases} \tag{B2}$$

where $\chi(s)$ is the wave function of the electron and positron; (θ_1, φ_1) are the azimuth angles opened by the three-vector momentum,

$$\chi\left(+\frac{1}{2}\right) = \begin{pmatrix} \cos\frac{\theta_1}{2} \\ \sin\frac{\theta_1}{2} e^{i\varphi_1} \end{pmatrix}, \qquad \chi\left(-\frac{1}{2}\right) = \begin{pmatrix} -\sin\frac{\theta_1}{2} e^{-i\varphi_1} \\ \cos\frac{\theta_1}{2} \end{pmatrix}. \tag{B3}$$

APPENDIX C: USEFUL FORMULA

Started with the case of no form factor in the integral, Eq. (5) can be expressed as the power of the four-vector momentum of the exchange meson (p_2), and it is easy to show that the power of p_2 is no more than three. We apply the Feynman parameter dimensional regularization scheme to express the integral as a linear combination of the following forms:

$$\begin{aligned} &\int \frac{d^4p_2}{(2\pi)^4} \frac{p_2^\mu}{[(p_2 - p_\psi)^2 - m_1^2][p_2^2 - m_2^2][(p_2 + p_\eta^2) - m_3^2]} \\ &= \frac{i}{16\pi^2} \int dxdy \frac{-P^\mu}{M^2 - P^2}, \\ &\int \frac{d^4p_2}{(2\pi)^4} \frac{p_2^\mu p_2^\nu}{[(p_2 - p_\psi)^2 - m_1^2][p_2^2 - m_2^2][(p_2 + p_\eta^2) - m_3^2]} \\ &= \frac{i}{16\pi^2}\left[\int dxdy \frac{P^\mu P^\nu}{M^2 - P^2} + \frac{1}{4}\Gamma\left(\frac{\epsilon}{2}\right)\delta^{\mu\nu}\right], \\ &\int \frac{d^4p_2}{(2\pi)^4} \frac{p_2^\mu p_2^\nu p_2^\sigma}{[(p_2 - p_\psi)^2 - m_1^2][p_2^2 - m_2^2][(p_2 + p_\eta^2) - m_3^2]} \\ &= \frac{i}{16\pi^2}\left[\int dxdy \frac{-P^\mu P^\nu P^\sigma}{M^2 - P^2}\right. \\ &\quad \left. - \frac{1}{4}\Gamma\left(\frac{\epsilon}{2}\right)(\delta^{\mu\nu}P^\sigma + \delta^{\mu\sigma}P^\nu + \delta^{\nu\sigma}P^\mu)\right], \end{aligned} \tag{C1}$$

where $P = yp_\eta - xp_\psi$, $M^2 = x(p_\psi^2 - m_1^2) + y(p_\eta^2 - m_3^2) - (1 - x - y)m_2^2$; ϵ is an infinitesimal parameter. The details can be found in Refs. [33,34].

To cancel the divergence with a monopole form factor, we just replace the exchanged-meson mass by the cutoff energy Λ to obtain the transition amplitude since the divergent term is independent of the intermediate meson masses:

$$\mathcal{M}_{fi}^{\rm mo}(m_1, m_2, m_3, \Lambda) = \mathcal{M}_{fi}(m_1, m_2, m_3) - \mathcal{M}_{fi}(m_1, \Lambda, m_3),$$

where $\mathcal{M}_{fi}(m_1, m_2, m_3)$ denotes the amplitude of Eq. (5) with $\mathcal{F}(p_2^2) = 1$.

For the case of a dipole form factor, we use the identity

$$\left(\frac{\Lambda^2 - m^2}{\Lambda^2 - p^2}\right)^2 = \lim_{\delta\to 0} \frac{\Lambda^2 - m^2}{\Lambda^2 - p^2} \frac{(\Lambda + \delta)^2 - m^2}{(\Lambda + \delta)^2 - p^2}, \tag{C2}$$

to have

$$\mathcal{M}_{fi}^{\rm di}(m_1, m_2, m_3, \Lambda) = \mathcal{M}_{fi}^{\rm mo}(m_1, m_2, m_3, \Lambda) + \lim_{\delta\to 0} \frac{m_2^2 - \Lambda^2}{2\Lambda\delta} \times \mathcal{M}_{fi}^{\rm mo}(m_1, \Lambda, m_3, \Lambda + \delta).$$

[1] K. Abe *et al.* (Belle Collaboration), Phys. Rev. Lett. **89**, 142001 (2002).
[2] K. Abe *et al.* (Belle Collaboration), Phys. Rev. D **70**, 071102 (2004).
[3] B. Aubert *et al.* (*BABAR* Collaboration), Phys. Rev. D **72**, 031101 (2005).
[4] G. T. Bodwin, E. Braaten, and G. P. Lepage, Phys. Rev. D **51**, 1125 (1995); **55**, 5853(E) (1997).
[5] E. Braaten and J. Lee, Phys. Rev. D **67**, 054007 (2003); **72**, 099901(E) (2005).
[6] K. Y. Liu, Z. G. He, and K. T. Chao, Phys. Lett. B **557**, 45 (2003).

[7] K. Hagiwara, E. Kou, and C. F. Qiao, Phys. Lett. B **570**, 39 (2003).
[8] Y. J. Zhang, Y. J. Gao and K. T. Chao, Phys. Rev. Lett. **96**, 092001 (2006).
[9] G. T. Bodwin, D. Kang, and J. Lee, Phys. Rev. D **74**, 014014 (2006).
[10] G. T. Bodwin, D. Kang, T. Kim, J. Lee, and C. Yu, AIP Conf. Proc. **892**, 315 (2007).
[11] G. T. Bodwin, J. Lee, and C. Yu, Phys. Rev. D **77**, 094018 (2008).
[12] Z. G. He, Y. Fan, and K. T. Chao, Phys. Rev. D **75**, 074011 (2007).
[13] B. Gong and J. X. Wang, Phys. Rev. D **77**, 054028 (2008).
[14] A. E. Bondar and V. L. Chernyak, Phys. Lett. B **612**, 215 (2005).
[15] J. P. Ma and Z. G. Si, Phys. Rev. D **70**, 074007 (2004).
[16] V. V. Braguta, A. K. Likhoded, and A. V. Luchinsky, Phys. Rev. D **72**, 074019 (2005).
[17] V. V. Braguta, A. K. Likhoded, and A. V. Luchinsky, Phys. Lett. B **635**, 299 (2006).
[18] X. H. Guo, H. W. Ke, X. Q. Li, and X. H. Wu, arXiv:0804.0949.
[19] H. Y. Cheng, C. K. Chua, and A. Soni, Phys. Rev. D **71**, 014030 (2005).
[20] X. Liu, X. Q. Zeng, and X. Q. Li, Phys. Rev. D **74**, 074003 (2006).
[21] G. Li, Q. Zhao, and B. S. Zou, Phys. Rev. D **77**, 014010 (2008).
[22] G. Li, Y. J. Zhang, and Q. Zhao, arXiv:0803.3412.
[23] G. Li and Q. Zhao, arXiv:0709.4639.
[24] H. J. Lipkin, Nucl. Phys. **B291**, 720 (1987).
[25] H. J. Lipkin, Phys. Lett. B **179**, 278 (1986).
[26] K. Abe *et al.* (Belle Collaboration), Surv. High Energy Phys. **18**, 221 (2003).
[27] A. Deandrea, G. Nardulli, and A. D. Polosa, Phys. Rev. D **68**, 034002 (2003).
[28] Y. Oh, W. Liu, and C. M. Ko, Phys. Rev. C **75**, 064903 (2007).
[29] Y. Jia, Phys. Rev. D **76**, 074007 (2007).
[30] W. M. Yao *et al.* (Particle Data Group), J. Phys. G **33**, 1 (2006).
[31] T. Bauer and D. R. Yennie, Phys. Lett. B **60**, 169 (1976).
[32] G. T. Bodwin, X. Garcia i Tormo, and J. Lee, arXiv:0805.3876.
[33] A. Denner, Fortschr. Phys. **41**, 307 (1993).
[34] T. Hahn and M. Perez-Victoria, Comput. Phys. Commun. **118**, 153 (1999).